Simulation of beam-beam effects in a circular e^+e^- collider

Kazuhito Ohmi
KEK, High Energy Accelerator Research Organization, Tsukuba, Ibaraki 305-0801, Japan
(Received 11 January 2000)

We have carried out a strong-strong simulation to study the beam-beam effect in a circular electron-positron collider. In the simulation, both the positron and electron beams are represented by macroparticles, and the interaction between the two beams is obtained by solving the Poisson equation for the charge distribution of the macroparticles. Using the simulation, we investigate the beam-beam limit and the coherent beam-beam tune shift, two characteristic phenomena of the beam-beam effect. We also study collision with a finite crossing angle, and verify its feasibility for the KEKB factory. Our results for KEKB yield an estimated luminosity of 8.5×10^{33} $\mathrm{cm}^{-2}\,\mathrm{s}^{-1}$, only slightly lower than the design value of 1×10^{34} $\mathrm{cm}^{-2}\,\mathrm{s}^{-1}$.

PACS number(s): 29.20.Dh, 29.27.−a, 41.75.Ht

I. INTRODUCTION

Particle factories, which produce B, charmonium, or ϕ mesons with high statistics, require high luminosities ($>10^{33}$ $\mathrm{cm}^{-2}\,\mathrm{s}^{-1}$). They are designed to run at a high beam-beam parameter and at a low single bunch current, and to achieve the luminosity by using many bunches. In such colliders the beam-beam limit can be reached without encountering single bunch collective phenomena, like the head-tail effect and bunch lengthening, i.e., it is the beam-beam effect that limits the luminosity. It is therefore important to study the beam-beam effect for such machines quantitatively.

Computer simulations are necessary to quantitatively study the beam-beam effect, since the interaction between two colliding beams is highly nonlinear. Much work has been done on this topic using various types of computer programs. These can roughly be classified into three kinds of methods: the rigid bunch model, weak-strong simulations, and strong-strong simulations. The rigid bunch model, the simplest of the three, has been used to study the coherent mode of the two beam system [1]. The weak-strong simulation, which is generally used to design colliders [2–5], can be used to predict the luminosity and the formation of non-Gaussian halos quantitatively, though coherent effects cannot be addressed. Finally the strong-strong simulation, which is not as established as the other two methods, has been used by Krishnagopal [6,7] to study the flip-flop effect and beam size oscillations in CESR and PEP-II.

The strong-strong simulation, which requires large amounts of computer resources, has recently become feasible due to the fast progress in computing power during the 1990s. In a strong-strong simulation both colliding beams are represented by macroparticles. A large number of macroparticles is used in order to reduce the effect of statistical noise. The electromagnetic field of each relativistic beam is obtained by solving the two-dimensional Poisson equation, which we here solve using the particle-in-cell (PIC) method. On each turn the electromagnetic fields are calculated for both e^- and e^+ beams, and then these beams are allowed to interact with each other through the fields.

Let us discuss the beam-beam limit and the coherent beam-beam tune shift which are essential issues for understanding the beam-beam effect. The beam-beam limit is a luminosity saturation phenomenon observed in high intensity collisions. For two Gaussian bunches in collision, the luminosity L is expressed

$$L=\frac{n^+n^-f_c}{2\pi\bar{\sigma}_x\bar{\sigma}_y},\quad \bar{\sigma}_i=\sqrt{\sigma_{i,+}^2+\sigma_{i,-}^2}, \tag{1}$$

where $n^\pm$ is the number of particles in a bunch, f_c the collision frequency, and $\sigma_{x,y}^\pm$ the bunch size. Note that $+/-$ are used to indicate the properties of the e^+/e^- beam. Here the longitudinal structure of the beam has been neglected. Equation (1) shows that the luminosity is proportional to n^+n^-, if the beam sizes are kept constant.

The beam-beam parameter ξ is used as a measure of the strength of the beam-beam effect. It is given by

$$\xi_{x,y}^\pm=\frac{n^\mp r_e}{\gamma^\pm}\,\frac{\beta_{x,y}^\pm}{2\pi\sigma_{x,y}^\mp(\sigma_x^\mp+\sigma_y^\mp)}, \tag{2}$$

where $r_e=2.82\times10^{-15}$ m is the classical electron radius, and $\beta^\pm$ and $\gamma^\pm$ are the beta function and relativistic factor, respectively, of the $e^\pm$ beam. The beam-beam parameter $\xi^\pm$ equals the incoherent tune shift of the $e^\pm$ beam due to the interaction with the opposing beam ($e^\mp$). There are four beam-beam parameters: for electrons and/or positrons and for the horizontal and/or vertical plane. Note that the beam-beam parameter of each beam linearly depends on the current of the opposing beam. We will use the same definition of the beam-beam parameter ξ when considering collisions with a finite crossing angle in Sec. V. In such collisions the incoherent tune shift becomes somewhat less than the beam-beam parameter.

Experimentally the luminosity is found to be proportional to n_+n_- at low currents, then grows more slowly at higher currents, and finally reaches a limit where the tune shift is ~0.05. We call this limit the beam-beam limit.

Another issue, the coherent beam-beam tune shift is relevant to the coherent motion of the two colliding beams. The beams can be considered as two oscillators, each with its own eigenfrequency (tune). The two oscillators (beams) couple with each other through the beam-beam interaction.

Suppose that the two beams have the same tune. These two degenerate modes split into two modes with different eigentunes due to the beam-beam interaction. The eigenmodes can be represented by mixed states of the two beams. The two modes are called the σ and π modes, respectively, representing the case in which the two beams have the same betatron phase, and the case where there is a phase difference of π, respectively. Note that the tune of the π mode is larger than that of the σ mode by $\sim\xi$ [1]. These coherent modes have been observed in experiments [8].

In recently constructed e^+e^- colliders, bunches fill many rf buckets in order to obtain a high luminosity. A higher luminosity requires a reduced bunch spacing, with the result that beam collision with a finite crossing angle has been proposed and studied [5]. Several colliders have been designed and constructed with the crossing angle on the basis of such studies, and have now begun their commissioning [9,10]. Up to now the luminosity of colliders with a finite crossing angle has been studied using only weak-strong simulations. In this paper we perform strong-strong simulations for beam-beam collisions with a finite crossing angle and investigate the reliability of machine performance for such a configuration.

We begin, in Sec. II, by presenting our model of the strong-strong simulation. In Secs. III and IV we discuss the beam-beam limit and the beam-beam tune shift, respectively. In these sections we limit ourselves to two-dimensional simulations to study the phenomena. Finally, in Sec. V we present results of three-dimensional simulations for a collider with a finite crossing angle.

II. MODEL OF SIMULATION

In the strong-strong simulation, the calculation of the beam-beam force is the most important issue. The calculation has to be performed rapidly and accurately for beams with arbitrary distributions. The simulation, in which the calculation of the beam-beam force is performed twice in every collision, should be continued for several radiation damping times in order to allow the system to reach a steady state. Symplecticity of the force will be important for long term stability. The study of the coherent motion of two beams is one of our goals; therefore, the number of macroparticles needs to be significantly large in order to distinguish coherent motion from statistical noise.

In our study the colliding $e^{\pm}$ beams are assumed to be ultrarelativistic ($\gamma^{\pm}\gg 1$). We use as a dynamical variable, $\boldsymbol{x}(s)=(x,p_x,y,p_y,z,p_z)$, which is generally used to describe beam motion in accelerators: $p_{x,y}$ is the transverse momentum normalized by the total momentum of a reference particle ($p_0=E_0/c$), z is the delay time ($z=s-ct$) scaled by the light speed, and p_z is the energy deviation [$p_z=(E-E_0)/E_0$] from that of the reference particle. Here s, which is the longitudinal coordinate, is treated as a timelike variable in the motion. The collision point is denoted by s^*.

The electric and magnetic fields produced by relativistic charged particles are evaluated by solving a two-dimensional electrostatic problem, because the strength and direction of the electric force is equal to that of the magnetic force. The electrostatic potential ($\phi^{\pm}$) due to the $e^{\pm}$ beam obeys the two-dimensional Poisson equation

$$\Delta_2\phi^{\pm}(\boldsymbol{r})\equiv\left(\frac{\partial^2}{\partial x^2}+\frac{\partial^2}{\partial y^2}\right)\phi^{\pm}(\boldsymbol{r})=-\frac{\rho^{\pm}(\boldsymbol{r})}{\epsilon_0}, \tag{3}$$

where $\rho^{\pm}$ is the charge distribution of $e^{\pm}$ beam and $\boldsymbol{r}=(x,y)$. The beam-beam force due to the $e^{\mp}$ beam is evaluated from the potential as follows:

$$\Delta p_x^{\mp}=-\frac{e}{p_0}\frac{\partial\phi^{\pm}(\boldsymbol{r})}{\partial x},\quad \Delta p_y^{\mp}=-\frac{e}{p_0}\frac{\partial\phi^{\pm}(\boldsymbol{r})}{\partial y}. \tag{4}$$

The solution of the Poisson equation is expressed as an integral over the Green function,

$$\phi(\boldsymbol{r})=-\frac{1}{2\pi\epsilon_0}\int d\boldsymbol{r}'G(\boldsymbol{r}-\boldsymbol{r}'),\quad \rho(\boldsymbol{r}'),\quad G(\boldsymbol{r})=\ln|\boldsymbol{r}|. \tag{5}$$

We use the discrete fast Fourier transform (FFT) in two-dimensional space to perform the integral. The transverse region containing the beam particle distribution is meshed ($n_x\times n_y$), and $G(\boldsymbol{r})$ and $\rho(\boldsymbol{r})$ are projected onto the mesh. In the projection of ρ, the charge of macroparticles (x,y) is deposited on the mesh points with a weight function $w_{ij}(x,y)=(1-|x-x_i|/\Delta x)(1-|y-y_j|/\Delta y)$, where (x_i,y_j) denotes the nearest four mesh points of (x,y) and $\Delta x(y)$ is mesh size. We do not consider particles outside of the $n_x\times n_y$ rectangle in the present simulation. The meshed region should be chosen with a margin so that macroparticles do not go out of the region. We have to be careful in this regard when a strong beam blow up is caused by the beam-beam interactions. The FFT's of $G(\boldsymbol{r})$ and $\rho(\boldsymbol{r})$ are evaluated, and their convolution gives the potential, i.e.,

$$\hat{\rho}(\boldsymbol{k})=\int\rho(\boldsymbol{r})\exp(i\boldsymbol{k}\cdot\boldsymbol{r})d\boldsymbol{r}, \tag{6}$$

$$\hat{G}(\boldsymbol{k})=\int G(\boldsymbol{r})\exp(i\boldsymbol{k}\cdot\boldsymbol{r})d\boldsymbol{r}, \tag{7}$$

$$\phi(\boldsymbol{r})=-\frac{1}{2\pi\epsilon_0}\frac{1}{(2\pi)^2}\int\hat{G}(\boldsymbol{k})\hat{\rho}(\boldsymbol{k})\exp(-i\boldsymbol{k}\cdot\boldsymbol{r})d\boldsymbol{k}. \tag{8}$$

The Green function $\ln|\boldsymbol{r}|$ has a singularity at the origin $\boldsymbol{r}=0$, but its integral is regular. The Green function is integrated for each mesh cell of area $\Delta x\times\Delta y$, and then is transformed into $\boldsymbol{k}$ space,

$$G(x_i,y_j)=\int_{y_j-\Delta y/2}^{y_j+\Delta y/2}\int_{x_i-\Delta x/2}^{x_i+\Delta x/2}G(x,y)dx\,dy, \tag{9}$$

$$\hat{G}(k_l,q_m)=\sum_{i,j=1}^{n_x,n_y}G(x_i,y_j)\exp(ik_lx_i+iq_my_j). \tag{10}$$

The integral Eq. (9) is performed numerically for each mesh cell. The integrand is evaluated $10(x)\times 10(y)=100$ times inside the region $\Delta x\times\Delta y$. The integration error is 0.7% for the mesh point nearest to the origin, and rapidly decreases

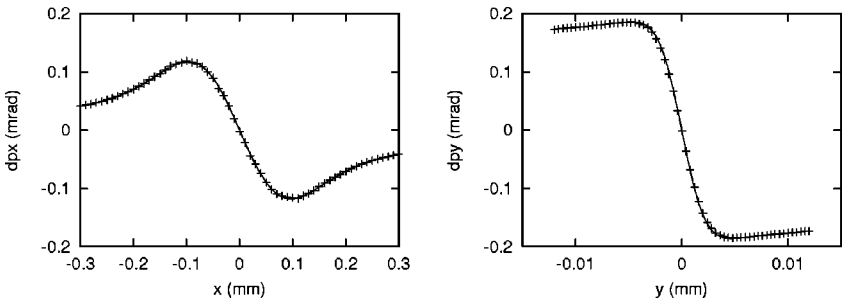

FIG. 1. Beam-beam force calculated by an electric potential due to a Gaussian beam. 100 000 particles are generated in a Gaussian distribution. The solid line shows the force calculated by the Bassetti-Erskine formula.

away from the origin.[1] To evaluate Eq. (5) for nonperiodic functions on the meshed space, $\rho(\boldsymbol{r})$ and $G(\boldsymbol{r})$, we use a $2n_x \times 2n_y$ mesh and put macroparticles in only an $n_x \times n_y$ region [12]. This method is generally used to treat a potential problem for an isolated system [$\phi(\infty) \rightarrow$ const]. The potential, which is given only on the mesh points, can be interpolated to other points using spline fitting; that is, the spline functions (first and second derivatives) are calculated on all the mesh points globally and the potential is estimated by bicubic interpolation [11], so that the first and second derivatives of the potential are continuous everywhere. The symplectic condition is guaranteed by the relation,

$$\frac{\partial^2 \phi(\boldsymbol{r})}{\partial x \partial y} = \frac{\partial^2 \phi(\boldsymbol{r})}{\partial y \partial x} \tag{11}$$

because of the Poisson bracket $\{p_x, p_y\} = 0$. Note that the Laplacian of ϕ ($\triangle_2 \phi$) is a continuous function of $\boldsymbol{r}$.

If the particle distribution is Gaussian, the potential and the force can be represented analytically, with the force given by the Bassetti-Erskine (BE) formula [13]. We have checked the solution of our Poisson solver for a Gaussian distribution by comparing the result with the force given by the BE formula. Figure 1 shows the beam-beam force along the x and y axes, as given by our program (the plotting symbols) and by the BE formula (the solid curve). We see good agreement.

The strong simulation is performed by combining the results of the Poisson solver and of a transfer map for one ring revolution. The actual calculation is carried out along the following steps.

(1) *Initialization.* We first generate macroparticles with a Gaussian distribution in six-dimensional phase space. The initial emittances of the beam are set to be their nominal values.

(2) *Beam-beam kick.* The electric potential and force due to the two beams are calculated by using the method described above, and then the macroparticles of each beam are kicked by the potential of the opposing beam.

(3) *One turn map through the ring.* We consider only the linear map for the revolution of particles, because we here are concerned only with the core distribution of the beam. The macroparticle coordinates in both beams are transferred by multiplying by the revolution matrix M, with 6×6 components,

$$\boldsymbol{x}(s^* + C) = M\boldsymbol{x}(s^*), \tag{12}$$

where C is the circumference of the ring.

(4) *Radiation damping and quantum excitation.* Radiation damping and quantum excitation are evaluated at only one position in the ring, the interaction point. On the normal mode X_i of M, the transformation is expressed as follows [14]:

$$X_i = X_i(1 - D_i), \tag{13}$$

$$X_i = X_i + \sqrt{2\varepsilon_i D_i}\hat{F}, \tag{14}$$

where $D_i = T_0/\tau_i$ is damping rate in one revolution (T_0 is the revolution time, τ_i is the damping time), and $\hat{F}$ is a Gaussian random variable with unit variance.

(5) *The transverse wake force and chromaticity.* We may also take into account the transverse wake force and chromaticity depending on operating parameters. The code includes their effects by a single kick,[2]

$$H_c = \left(\frac{\pi \xi_x}{\beta_x} x^2 + \frac{\pi \xi_y}{\beta_y} y^2 \right) p_z, \tag{15}$$

$$H_w = \frac{n^{\pm} e^2}{E} \{F_x(z)x + F_y(z)y\}, \tag{16}$$

where $F_i(z)$ is the convolution of the dipole moment of beam and the transverse wake force [15]. We have found that, with our parameters, these effects influence the results only weakly, though they are interesting scientifically. We will no longer mention these effects in this paper.

After initialization (1), we repeat the sequence [(2)–(4) or (5)] for a period of several radiation damping times.

The luminosity is calculated using the definition

$$L = f_0 \int ds\, dz\, dz' \int dx\, dy\, \rho^+(x,y,z,s)\rho^-(x,y,z',-s) \times \delta(s - (z - z')/2), \tag{17}$$

[1]The integral is replaced with the exact solution, $\int\int \ln(x^2 + y^2)dx\, dy = -3xy + x^2 \tan^{-1}(y/x) + y^2 \tan^{-1}(x/y) + xy \log(x^2 + y^2)$ in the latest version of the code.

[2]The chromaticity kick is not unique. The Hamiltonian is determined by giving the momentum dependence of the β function at the interaction point for more accurate treatment.

TABLE I. Basic parameters of KEKB.

	HER	LER
Particle	e^-	e^+
C	3016 m	
E	8 GeV	3.5 GeV
I	1.1A	2.6A
N_{bunch}	$\sim$5000	
$n_{e,p}$/bunch	1.4×10^{10}	3.3×10^{10}
β_x	0.33 m	
β_y	0.008 m	
ε_u	1.8×10^{-8} m	
ε_v	3.6×10^{-10} m	
$\xi^{\pm}_{x,y}$	$\sim$0.059	
ν_x/ν_y	0.52/0.08	
$T_0/\tau_{xy,z}$	$2.5/5.0\times10^{-4}$	$1.2/2.4\times10^{-4}$
θ_c	2×11 mrad	

where $\rho^{\pm}(x,y,z)$ is density of the $e^{\pm}$ beam. The integration is evaluated by summing the macroparticle density on the mesh points.

We use this simulation to study the beam-beam effect in the KEKB facotry (KEKB). KEKB is an asymmetric circular collider, which consists of a low energy positron ring (LER) and a high energy electron ring (HER). The parameters for KEKB which are important for the beam-beam effect are shown in Table I.

We first show the dependence on the statistics and the mesh size in a typical example. Three trials with different statistics and mesh size are given in Table II.[3] The number of mesh points (n_x and n_y) is that of real space where the macroparticles are mapped. A FFT is performed in $2n_x\times2n_y$ mesh space, as was mentioned before. Their results are consistent with each other. Hereafter we use a 64×64 mesh with a horizontal and vertical size of 10×0.4 μm^2, respectively, and take $N=100\,000$.

III. BEAM-BEAM LIMIT

We discuss here the beam-beam limit using the strong-strong simulation. The beam-beam limit was studied by doing simulations for various stored currents ($n^{\pm}$). The bunch population of the two beams was varied between 20%–140% of the design value, corresponding to a beam-beam parameter $0.012\leqslant\xi_y\leqslant0.083$. In our simulations the condition, $n^+/n^-=\gamma^-/\gamma^+$, is always kept; therefore the beam-beam parameter is often used in place of the beam current hereafter. The beam sizes, the barycenter, and the luminosity were calculated on every turn.

Figure 2 shows the evolution of the beam sizes ($\sigma_{x,y}$) and the luminosity (L) for various beam-beam parameters. The figure shows that an equilibrium is reached at around 20 000 turns except for calculations using two parameters, $\xi=0.0472$ and 0.0533. The different curves in the figure give results for beam-beam parameters, $\xi=0.0356$, 0.0415, 0.0472, 0.0533, and 0.0593. Results for $\xi<0.0356$ and $\xi>0.0593$ are rather smooth, e.g., $\sigma_{x,y}$ for $\xi<0.0356$ is roughly constant, and that at $\xi>0.0593$ increases monotonically for ξ. The figure shows that the vertical beam size and luminosity fluctuate at $\xi=0.0415$ and 0.0472, and the luminosity for $\xi=0.0472$ is larger than that of 0.0533, i.e., an inversion of luminosity occurs.

TABLE II. Check for statistics and mesh size.

N	50 000	50 000	100 000
Mesh	64×64	128×128	64×64
Mesh size (μm)	10×0.4	5×0.3	10×0.4
L	8.7×10^{33}	8.4×10^{33}	8.6×10^{33}
$\sigma_x(\mu\text{m})e^-/e^+$	63/66	63/64	62/67
$\sigma_y(\mu\text{m})e^-/e^+$	2.4/4.2	2.4/4.4	2.3/4.4

It is helpful to see the dipole motion to understand the luminosity behavior. Figure 3 shows the evolution of the vertical dipole amplitude for various ξ. We find that clear coherent vertical motion occurs for $\xi\geqslant0.0593$ [see Figs. 3(g)–3(i)]. For $\xi=0.0593,0.0652$ [see Figs. 3(g) and 3(h)], the dipole motion dies out with time, while the beam size enlarges initially and stays large [for $\xi=0.0593$ as seen in Figs. 2(c) and 2(d)]. The fall off of the dipole coherent mode may be due to filamentation of the motion due to an amplitude-dependent tune in the strong nonlinear force at large amplitude (around $y=0.2$ μm). The beam loses a dipole-type coherence, but retains its large vertical extent after the initial big displacement. On the other hand, at $\xi=0.0771$ the dipole amplitude falls off only slowly, which suggests that this simple picture is not the whole story. Note that the amplitude of the dipole motion is not very large: it reaches to only $\sim$10% of the natural beam size at its maximum. The dipole amplitude appears to grow beginning with $\xi=0.0415$ [see Fig. 3(d)]. The amplitude continues to increase and displays a clear dipole signal beginning with ξ

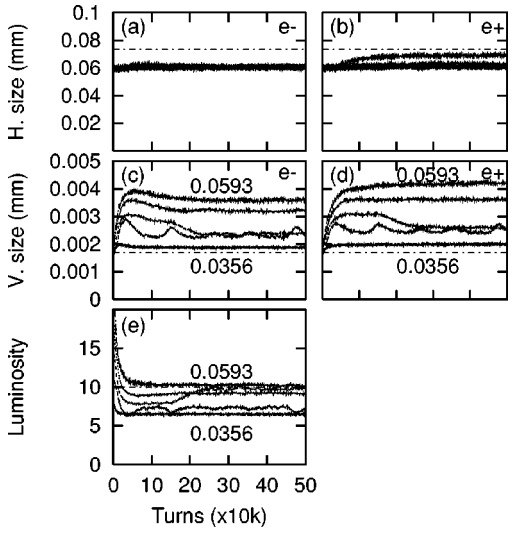

FIG. 2. Evolution of $\sigma_y(e^-)$, $\sigma_y(e^+)$, and luminosity for beam-beam parameters $\xi=0.0356,0.0415,0.0472,0.0533,0.0593$. Dashed lines give the nominal values. Luminosity is plotted in units of 10^{33} cm^{-2} s^{-1}.

[3]These results are obtained for three-dimensional simulation with a crossing angle, which is discussed in Sec. V.

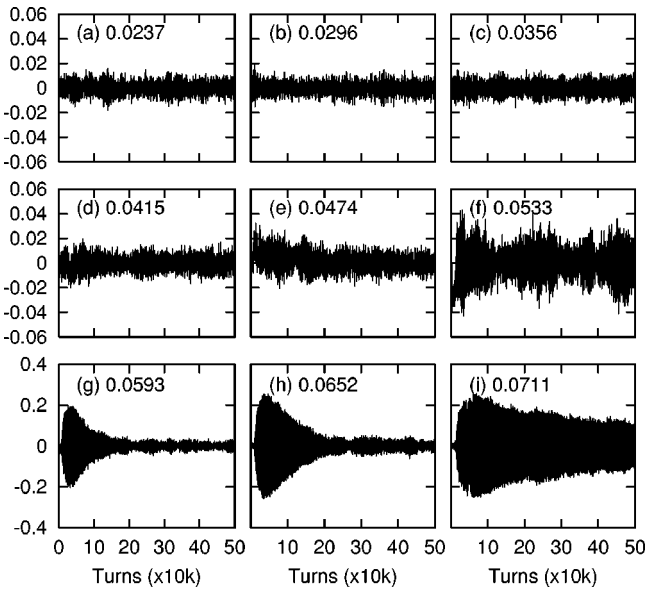

FIG. 3. Evolution of the vertical dipole amplitude of the e^+ beam. Vertical axes give the vertical amplitude in units of μm. The corresponding beam-beam parameter is written in each figure.

$=0.0593$ [Fig. 3(g)]. We may conclude that the region of $\xi = 0.04$–0.05 is near the threshold of the dipole instability. This progression of plots illustrates the phenomenon of the beam-beam limit well.

The relation of the final beam sizes to the luminosity as a function of ξ is shown in Fig. 4. The dotted lines show the natural beam sizes and the geometrical luminosity. The horizontal beam size of the $e^\pm$ beam decreases with increasing ξ at $\xi<0.05$. This is due to the dynamic beta effect; that is, the focusing force due to the beam-beam interaction increases or

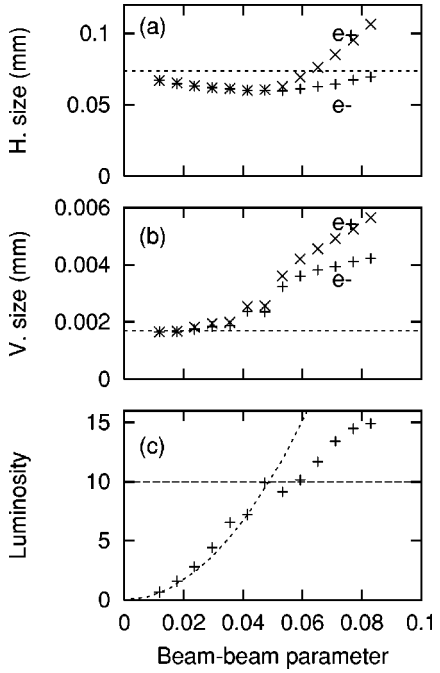

FIG. 4. Beam sizes and luminosity for various currents. Dashed lines show the nominal values. Luminosity is plotted in units of 10^{33} cm^{-2} s^{-1}.

decreases the effective β function depending on the betatron tune. For $\xi>0.05$, σ_x begins to increase. The size of the electron beam remains smaller than the natural size, while that of the positron beam becomes larger than the natural size. The vertical beam size is about the natural size for $\xi<0.04$, while it enlarges for higher ξ, with the enlargement of the positron beam more pronounced than that of the electron beam. This difference in behavior is due to the difference of the two damping times: that of the electron beam is half that of the positron beam (see Table I). The luminosity increases quadratically for $\xi<0.05$, while it increases more slowly at higher currents.

IV. COHERENT BEAM-BEAM TUNE SHIFT

Consider two opposing beams with the same tune. When coupled through the beam-beam force the two eigenmodes will have different tunes. The coherent beam-beam tune shift is defined as the tune difference between the two eigenmodes.

We summarize the linear theory of a one-dimensional model for the coherent tune shift [1]. The two beams are assumed to be rigid bunches with Gaussian distributions. The two beams are considered to be a coupled, two-oscillator system connected by the beam-beam force. The beam-beam force is linearized and is expressed as

$$\Delta p^\pm = -\frac{2\pi\xi^\pm}{\beta^\pm}(y^\pm - y^\mp). \tag{18}$$

The coordinates of the two beams are transferred by the beam-beam force and one revolution through the ring as follows:

$$\begin{pmatrix} \boldsymbol{Y}^+(s+C) \\ \boldsymbol{Y}^-(s+C) \end{pmatrix} = KM \begin{pmatrix} \boldsymbol{Y}^+(s) \\ \boldsymbol{Y}^-(s) \end{pmatrix},$$
$$\boldsymbol{Y}^\pm(s) = \sqrt{n^\pm \gamma^\pm} \begin{pmatrix} y^\pm(s)/\sqrt{\beta^\pm} \\ p_y^\pm \sqrt{\beta^\pm} \end{pmatrix}, \tag{19}$$

where K, the transfer matrix for the linearized beam-beam force, is given by

$$K = \begin{pmatrix} 1 & 0 & 0 & 0 \\ -2\pi\xi^+ & 1 & 2\pi\sqrt{\xi^+\xi^-} & 0 \\ 0 & 0 & 1 & 0 \\ 2\pi\sqrt{\xi^+\xi^-} & 0 & -2\pi\xi^- & 1 \end{pmatrix}. \tag{20}$$

M is the revolution matrix for the two beams,

$$M = \begin{pmatrix} \cos 2\pi\nu_0 & \sin 2\pi\nu_0 & 0 & 0 \\ -\sin 2\pi\nu_0 & \cos 2\pi\nu_0 & 0 & 0 \\ 0 & 0 & \cos 2\pi\nu_0 & \sin 2\pi\nu_0 \\ 0 & 0 & -\sin 2\pi\nu_0 & \cos 2\pi\nu_0 \end{pmatrix}. \tag{21}$$

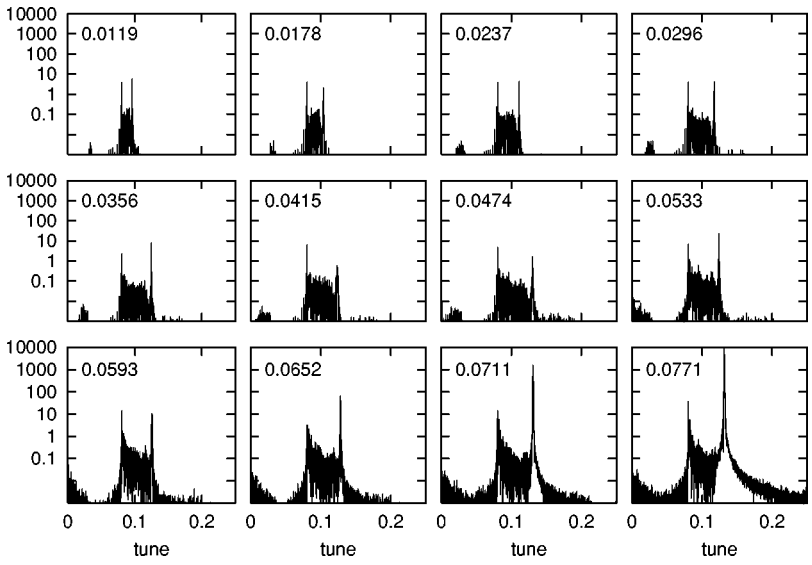

FIG. 5. Fourier spectra of the vertical dipole motion for various beam-beam parameters. The vertical axis is in arbitrary units. The corresponding beam-beam parameter is written in each figure.

The eigenvalues of the transfer matrix KM correspond to the tunes of the eigenmode, which are $\nu=\nu_0$ and $\nu=\nu_0+(\xi^+ +\xi^-)/2$. The eigenvectors are given by

$$\boldsymbol{Y}_\sigma=\boldsymbol{Y}^+ +\boldsymbol{Y}^-, \quad \boldsymbol{Y}_\pi=\boldsymbol{Y}^+ -\boldsymbol{Y}^-. \tag{22}$$

We see that the modes correspond to the correlated betatron motion of the two beams moving in phase and out of phase by π. These modes are called the σ and π modes, respectively. Note that the linear theory can be easily extended by allowing a different tune for each beam in Eq. (21).

These two eigenmodes have been observed in actual accelerators [8]. However, the measured tune difference between the two modes has been reported to be larger than $(\xi^+ +\xi^-)/2=\overline{\xi}$.

An analysis using the Vlasov equation can explain the enhancement of the beam-beam tune shifts observed [16]. The corrected tune shift is expressed by

$$\nu_\pi-\nu_0=G(r)\overline{\xi}, \quad r=\sigma_y/(\sigma_x+\sigma_y), \tag{23}$$

where

$$G=1.33-0.37r+0.279r^2, \quad \text{(horizontal)} \tag{24}$$

$$=1.33-0.37(1-r)+0.279(1-r)^2 \quad \text{(vertical)}. \tag{25}$$

The tune shifts for KEKB are estimated to be $\Delta\nu_x=1.32\overline{\xi_x}$ and $\Delta\nu_y=1.23\overline{\xi_y}$ by substituting $r=0.025$ ($\sigma_x=77$ μm, $\sigma_y=1.9$ μm).

We study this phenomena using the strong-strong simulation. Keeping $n^+\gamma^+\sim n^-\gamma^-$ implies that $\xi^+\sim\xi^-\sim\overline{\xi}$.

The data of the dipole amplitudes, which were shown in Fig. 3, are analyzed by performing a fast Fourier transform (FFT). Figure 5 shows the Fourier power spectra of the vertical dipole motion. In each case two peaks, which correspond to the tunes of the σ and π modes, are found. The distance between the two peaks is the coherent beam-beam tune shift. We see that the beam-beam tune shift increases gradually with increasing beam current (ξ) and that the Fourier amplitude of the π mode also grows at higher ξ. The coherent motion seen in Fig. 3 can be considered to be caused by the excitation of the π mode.

We have performed a similar analysis for the horizontal dipole motion. The relation of the beam-beam tune shift and the beam-beam parameter ξ is summarized in Fig. 6. The tune shift is evaluated using the relation,

$$\cos 2\pi\nu=\cos 2\pi\nu_0+2\pi\xi\sin 2\pi\nu_0. \tag{26}$$

We see that the vertical beam-beam tune shift linearly increases for $\xi<0.04$ and saturates at around $\xi\sim0.05$, while the horizontal tune shift increases linearly to higher ξ. The gradient of the vertical tune shift at lower currents is larger than the beam-beam parameter, and the horizontal shift is even larger. These features are consistent with experiment and the Vlasov theory.

V. THREE-DIMENSIONAL SIMULATION WITH CROSSING ANGLE

We have performed three-dimensional simulations of the beam-beam interaction with a finite crossing angle. The crossing angle is treated in accordance with Ref. [5]. Before collision, the macroparticles of the two beams are transferred to the head-on frame using a Lorentz boost. The transformation is given by

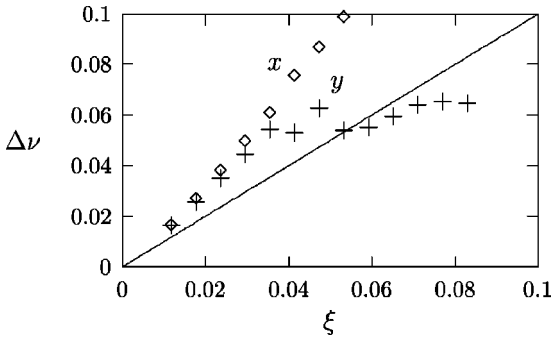

FIG. 6. Beam-beam tune shifts vs a nominal beam-beam parameter. Note that the straight line has a slope of 1.

$$x^* = \tan\phi z + \left(1 + \frac{p_x^*}{p_s^*}\sin\phi\right)x,$$

$$y^* = y + \sin\phi\frac{p_y^*}{p_s^*}x,$$

$$z^* = \frac{z}{\cos\phi} - \frac{H^*}{p_s^*}\sin\phi x,$$

$$p_x^* = \frac{p_x - \tan\phi H}{\cos\phi}, \tag{27}$$

$$p_y^* = \frac{p_y}{\cos\phi},$$

$$p_z^* = p_z - \tan\phi p_x + \tan^2\phi H,$$

where

$$H = (1+p_z) - \sqrt{(1+p_z)^2 - p_x^2 - p_y^2},$$

$$p_s = \sqrt{(1+p_z)^2 - p_x^2 - p_y^2}.$$

A star designates a dynamical variable in the head-on frame. Note that the x^* and y^* axes are defined in the same direction for both beams, while the s^* axis is defined in opposite directions, since the two beams travel in opposite directions.

The bunch is sliced in the longitudinal direction in the head-on frame. We consider the collision between the ith (e^+) and jth (e^-) slices which have longitudinal coordinates z_i^+ and z_j^-, respectively. Here i and j designate the slice number, counted from the head slice. The collision point between the two slices deviates by $\Delta s_{+,ij}^* = (z_i^+ - z_j^-)/2$ from the interaction point s^* in the coordinate of the e^+ beam. Since the sign of s is opposite for the e^+ and e^- beams, the deviation is expressed by $\Delta s_{-,ij}^* = -\Delta s_{+,ij}^*$ in the coordinate of the e^- beam.

All particles are transferred to the interaction point s^* before collision and are sorted into the slices. The slices are allowed to collide in the order $(i,j) = (1,1),(1,2),(2,1),(1,3),(2,2),(3,1),\ldots$. The particles, which collide at $\Delta s_{\pm,ij}^*$, are transferred to their collision point by [3]

$$\boldsymbol{X}_\pm = D_\pm(\Delta s_{\pm,ij}^*)\boldsymbol{x}_\pm,$$
$$D_\pm(\Delta s) \equiv \exp\left(:-\frac{p_{\pm,x}^2 + p_{\pm,y}^2}{2}\Delta s:\right), \tag{28}$$

where D is represented by the Lie operator, i.e., $:f(x,p):g(x,p) = \{f,g\}$ with $\{\}$ the Poisson bracket. The collision between the slices is performed as follows:

$$D_\pm(\Delta s_{\pm,ij}^*)\exp\left(:-\frac{e}{p_0}\phi_{\mp,i}^{\,j}(x_{\pm,j}^{\,i}, y_{\pm,j}^{\,i}):\right)D_\pm^{-1}(\Delta s_{\pm,ij}^*), \tag{29}$$

where $\phi_{-,j}$ and $\phi_{+,i}$ are the electric potential due to the jth electron and the ith positron slices, respectively. The beam-beam interaction in the head-on frame is carried out by repeating the transformation of Eq. (29) for all combinations of the slices. After the head-on collision, the macroparticles are transferred back to the unboosted frame by the inverse map of Eq. (27).

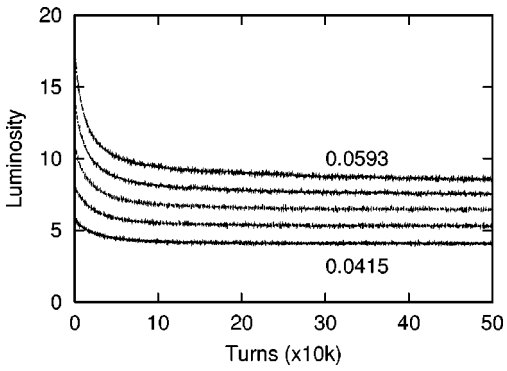

FIG. 7. Evolution of luminosity. The crossing angle is 2×11 mrad. Luminosity is plotted in units of 10^{33} cm^{-2} s^{-1}.

We have performed simulations in which both beams are represented by 100 000 macroparticles and for which five longitudinal slices are used. The macroparticles are tracked for 50 000 turns, while undergoing the interaction of the beam-beam force, the one turn map, and synchrotron radiation and quantum excitation. Results are similar to the two-dimensional ones given earlier. We find little enlargement in the horizontal beam sizes, and a large enlargement in the vertical beam sizes. The luminosity is reduced by the vertical enlargement. The beam sizes and luminosity are smooth function of ξ; we find no fluctuations. Figure 7 shows the time evolution of the luminosity for various beam-beam parameters ξ.

The final beam sizes and luminosity for various currents are summarized in Fig. 8. Here the beam-beam parameter is

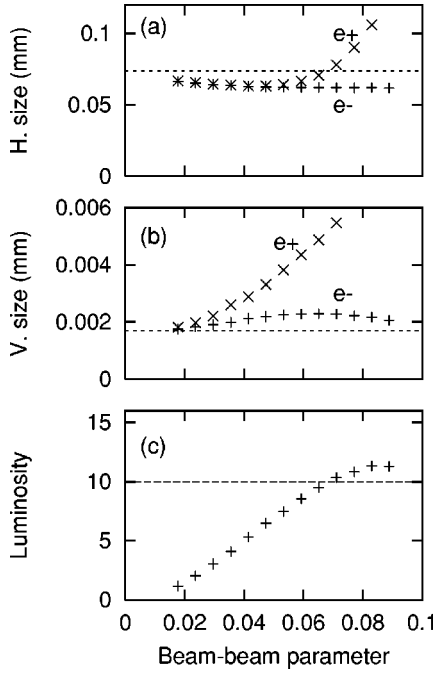

FIG. 8. σ_x, σ_y, and luminosity for various beam-beam parameters. The crossing angle is 2×11 mrad. Luminosity is plotted in units of 10^{33} cm^{-2} s^{-1}.

given by Eq. (2), and the incoherent beam-beam tune shift is about 90% of the beam-beam parameter due to the crossing angle [17]. The enlargement of the positron beam is enhanced compared to the case without a crossing angle, while that of the electron beam is reduced. The design value of the nominal beam-beam parameter is 0.059 for KEKB. The simulations show that a luminosity of 8.5×10^{33} $\mathrm{cm}^{-2}\,\mathrm{s}^{-1}$ can be achieved at this current. Note that this luminosity is slightly smaller than the design value of 1×10^{34} $\mathrm{cm}^{-2}\,\mathrm{s}^{-1}$.

VI. SUMMARY

We have studied the beam-beam effect in a circular e^+e^- collider using a strong-strong simulation program. The simulation makes it possible to consider beams with arbitrary distributions, since the beam-beam force is calculated by a Poisson solver using the particle in cell method. The beam-beam limit and coherent beam-beam tune shift were studied for the parameters of KEKB using a two-dimensional simulation.

The beam-beam limit phenomenon was seen in the current dependence of the luminosity. The simulation showed that the luminosity depends quadratically on the beam-beam parameter for $\xi<0.05$, with a somewhat weaker dependence on ξ at higher currents. In addition, it was shown that a vertical coherent motion, which corresponds to the π mode, is induced at higher values of the beam-beam parameter.

The coherent beam-beam tune shift was seen in the Fourier spectra of the beam dipole motion given in the simulations. It was found that the tune shift increases linearly with the beam current at lower currents, and saturates at higher currents. The slope of the tune shift dependence at lower currents is somewhat larger than predicted by the simple analytical estimate. The vertical tune shift saturated at $\xi_y \sim 0.05$ where the beam-beam limit occurs. We found, in addition, that the horizontal tune shift is larger than that of the vertical one, with a value consistent with the Yokoya factor.

A three-dimensional simulation with a finite crossing angle ($\theta_c=22$ mrad) was also carried out to study the feasibility of the KEKB factory design. The calculated luminosity is $\sim8.5\times10^{33}$ $\mathrm{cm}^{-2}\,\mathrm{s}^{-1}$, which is 85% of the KEKB design value.

ACKNOWLEDGMENTS

The author thanks K. Yokoya and K. Oide for many fruitful discussions concerning the algorithm of the strong-strong simulation. The author also thanks K. Bane for reading the manuscript.

[1] K. Hirata, Nucl. Instrum. Methods Phys. Res. A **269**, 7 (1988).
[2] S. Peggs and R. Talman, Phys. Rev. D **24**, 2379 (1981); A. Piwinski, IEEE Trans. Nucl. Sci. **NS-30**, 2378 (1983); G. Jackson and R. Siemann, Nucl. Instrum. Methods Phys. Res. A **286**, 17 (1990); S. Krishnagopal and R. Siemann, Phys. Rev. D **41**, 2312 (1990).
[3] K. Hirata, H. Moshammer, and F. Ruggiero, Part. Accel. **40**, 205 (1993).
[4] T. Chen, J. Irwin, and R. Siemann, Phys. Rev. E **49**, 2323 (1994); D. Shatilov, Part. Accel. **52**, 65 (1996).
[5] K. Hirata, Phys. Rev. Lett. **74**, 2228 (1995).
[6] S. Krishnagopal, Phys. Rev. Lett. **76**, 235 (1996).
[7] S. Krishnagopal, Phys. Rev. ST Accel. Beams **3**, 024401 (2000).
[8] H. Koiso *et al.*, Part. Accel. **27**, 83 (1990).
[9] K. Akai *et al.* (unpublished).
[10] M. Zobov (unpublished).
[11] W.H. Press *et al.*, *Numerical Recipies in Fortran 77*, 2nd ed. (Cambridge University Press, Cambridge,1992).
[12] R. W. Hockney and J. W. Eastwood, *Computer Simulation Using Particles* (Adam Hilger, Bristol, 1988); K. Oide and K. Yokoya (private communications); K. Yokoya, KEK Report No. 85-9 (1985).
[13] M. Bassetti and G. Erskine, CERN Report No. ISR TH/80-06 (1980).
[14] K. Ohmi, K. Hirata, and K. Oide, Phys. Rev. E **49**, 751 (1994).
[15] A. W. Chao, *Physics of Collective Beam Instabilities in High Energy Accelerators* (Wiley-Interscience, New York, 1993).
[16] K. Yokoya and H. Koiso, Part. Accel. **27**, 181 (1990).
[17] KEKB B-Factory design report, KEK Report No. 95-7 (1995).